Atmósfera (1990), **3**, pp. 203-216

A surface mesoscale wind model for complex terrain

MARIANO A. ESTOQUE

Clean Energy Research Institute, University of Miami, Coral Gables, Florida
and Dept. of Meteorology and Oceanography, University of the Philippines, Diliman, Quezon City, PHILIPPINES

(Manuscript received April 7, 1989, accepted in final form November 6, 1989)

RESUMEN

Se describe un modelo a mesoescala de la distribución del viento superficial sobre un terreno complejo, que está diseñado para simular las variaciones temporales y geográficas del campo de viento. Las ecuaciones del modelo incorporan los efectos de no uniformidad en la temperatura superficial, la rugosidad, y la elevación del terreno. Se han llevado a cabo integraciones iniciales de las ecuaciones del modelo para simular configuraciones de flujo en la vecindad de una colina aislada y sobre regiones costeras durante la ocurrencia de una brisa marina. Los resultados de las integraciones indican que el modelo es potencialmente útil para estudiar el flujo sobre terreno complejo

ABSTRACT

A mesoscale model of the surface wind distribution over complex terrain is described. It is designed to simulate the time as well as the geographical variations of the wind field. The model equations incorporate the effects of nonuniformities in surface temperature, roughness, and terrain elevation. Initial integrations of the model equations have been made to simulate flow patterns in the vicinity of an isolated hill and over coastal regions during the occurrence of a sea breeze. The results of the integrations indicate that the model is potentially useful for studying flow over complex terrain.

1. Introduction

Horizontal inhomogeneities of the Earth's surface generate smaller scale perturbations of the large-scale prevailing flows. In general, the important inhomogeneities consist of the following:

a. Variations in terrain elevation.

b. Variations in surface temperature.

c. Variations in surface roughness.

The perturbations which are generated may range from very small scale eddies (order of 1 cm in dimension) to mesoscale (horizontal dimensions of 1 km to 100 km) disturbances. Examples of such mesoscale circulations are land and sea breezes, mountain and valley winds, and the strong winds channelled through valleys.

Various models have been developed previously for simulating terrain-induced mesoscale circulations. These range in complexity from the simple one level or one layer models of Danard (1977), Mass and Dempsey (1985), and Lavoie (1972) to the complex multi-level, three-dimensional models of Pielke (1974), Estoque and Gross (1981) and others. As expected, the model simulations of the complex models are generally more accurate than the corresponding simulation of simpler models. However, simple models have the obvious advantage of requiring smaller computers for integrating the model equations.

The purpose of the present paper is to describe a simple, one-level model of terrain-induced mesoscale circulations. The approach in developing the model is similar to the one used in the above-mentioned models by Danard (1977) and of Mass and Dempsey (1985). There are, of course, some features of the present model which are different from those of the previous two; these will be noted in the description of the model which follows. Examples of simulation with the model will be presented.

2. The model equations

The model is a primitive equation model with a terrain-following coordinate in the vertical (σ) and the usual horizontal coordinates, x and y. The vertical coordinate is defined as:

$$\sigma \equiv \frac{Z - h}{D - h}$$

Here, Z is the height of a point, h is the height of the terrain, and D is the top of the physical model. The relationships among these different quantities are illustrated in Figure 1.

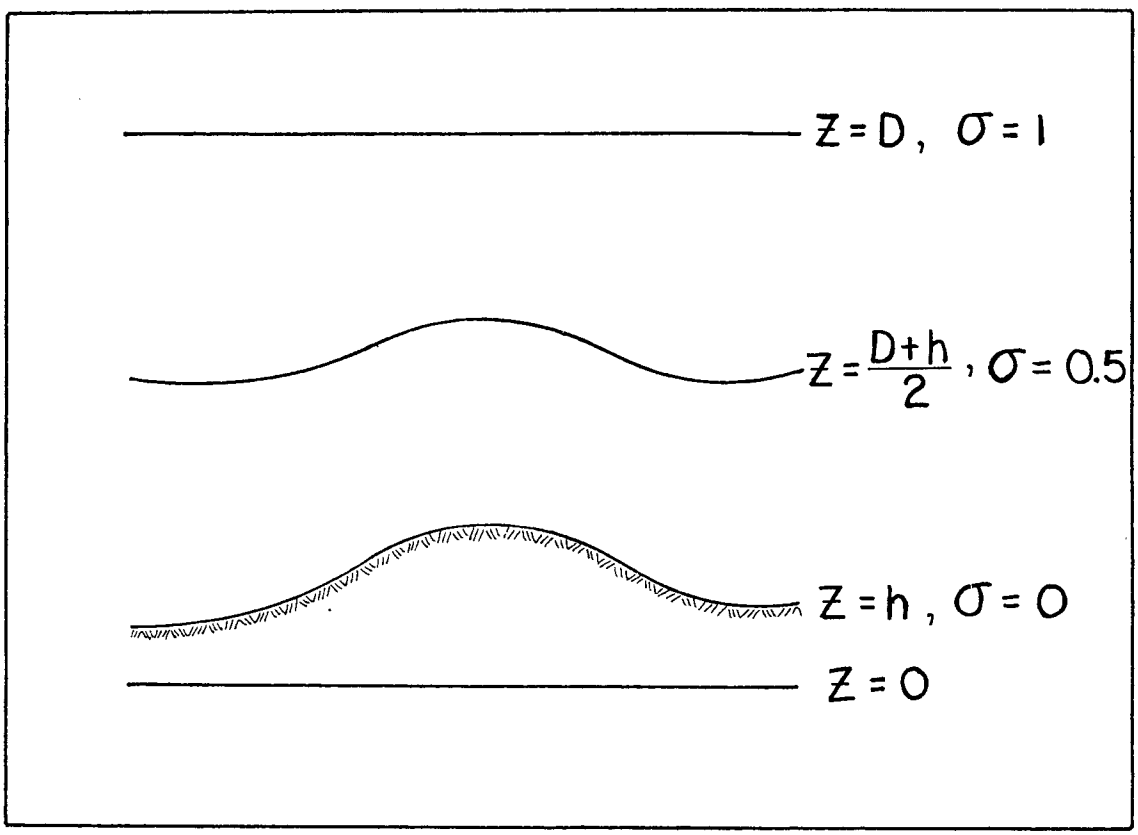

Fig. 1. Schematic diagram showing some characteristics of the vertical coordinate (σ).

The primary equations of the model are the momentum equations, the thermodynamic energy equation and the hydrostatic equation.

If applied at the surface (more precisely, at standard anemometer level), the first three equations may be written as follows:

$$\frac{\partial u}{\partial t} = -u\frac{\partial u}{\partial x} - v\frac{\partial u}{\partial y} + fv - \theta\frac{\partial \phi}{\partial x} - g\frac{\partial h}{\partial x} - K_1 u$$

$$-K_2(u - u_D) + \frac{\partial}{\partial x}(K_x\frac{\partial u}{\partial x}) + \frac{\partial}{\partial y}(K_y\frac{\partial u}{\partial y}) + (\frac{\partial u}{\partial t})_s \tag{1}$$

$$\frac{\partial v}{\partial t} = -u\frac{\partial v}{\partial x} - v\frac{\partial v}{\partial y} - fu - \theta\frac{\partial \phi}{\partial y} - g\frac{\partial h}{\partial y} - K_1 v$$

$$-K_2(v - v_D) + \frac{\partial}{\partial x}(K_x\frac{\partial v}{\partial x}) + \frac{\partial}{\partial y}(K_y\frac{\partial v}{\partial y}) + (\frac{\partial v}{\partial t})_s \tag{2}$$

$$\frac{\partial \theta}{\partial t} = -u\frac{\partial \theta}{\partial x} - v\frac{\partial \theta}{\partial y} + \frac{\partial}{\partial x}(K_x\frac{\partial \theta}{\partial x}) + \frac{\partial}{\partial y}(K_y\frac{\partial \theta}{\partial y})$$

$$+(\frac{\partial \theta}{\partial t})_R + (\frac{\partial \theta}{\partial t})_w + (\frac{\partial \theta}{\partial t})_Q \tag{3}$$

where u and v are the components of the velocity along x and y, θ is the potential temperature, f is the Coriolis parameter, and g is gravity. The quantities, u_D and v_D are the wind components at level D. The quantity ϕ is defined as follows:

$\phi = C_p(\frac{P}{P_o})^K$

$K = R/C_p$

R, gas content for air

C_p, specific heat at constant temperature

$P_o = 1000$ mb.

The hydrostatic equation is:

$$\frac{\partial \phi}{\partial \sigma} = -\frac{g}{\theta}(D - h) \tag{4}$$

In the two momentum equations, there are four physical processes which are parameterized, corresponding to the last five terms. These processes are:

1. Surface or skin friction: $K_1 u$, and $K_1 v$.
2. Momentum exchange between the surface and the upper level, D: $K_2(u - u_D)$, $K_2(v - v_D)$.
3. Horizontal diffusion of momentum:

$$\frac{\partial}{\partial x}(K_x\frac{\partial u}{\partial x}) + \frac{\partial}{\partial y}(K_y\frac{\partial u}{\partial x})$$

and

$$\frac{\partial}{\partial x}(K_x\frac{\partial v}{\partial x}) + \frac{\partial}{\partial y}(K_y\frac{\partial v}{\partial y})$$

4. Slope wind generation:

$$(\frac{\partial u}{\partial t}) \text{ and } (\frac{\partial v}{\partial t})_s$$

The first item above represents the tendency of ground friction to reduce the surface wind speed. The expression for the resistance coefficients, K_1, is given by:

$$K_1 \equiv C_D \mid V \mid /(D - h)$$

$$\mid V \mid = (u^2 + v^2)^{\frac{1}{2}}$$

The drag coefficient, C_D, depends on the thermal stability; the formula for C_D, is presented later in the text.

The second item represents the vertical exchange of momentum between the surface and the layers above. This produces the surface wind maximum during the daytime due to vertical mixing. The expression for K_2 is as follows:

$$K_2 = \frac{C_m V_D(1 - SRi)(1 + C_n\frac{h}{D})}{D}$$

where C_m, S, and C_n are empirical constants. The values of these constants and other model constants are given in Section 3. The quantity R_i is the Richardson number. The formula for the Richardson number is presented on a later page.

The third item represents the horizontal diffusion of momentum. The eddy diffusion coefficients, K_x and K_y, vary horizontally according to the formulas,

$$K_x = C_k(\Delta x)^2[(\frac{\partial u}{\partial x})^2 + (\frac{\partial v}{\partial x})^2]^{\frac{1}{2}}$$

$$K_y = C_k(\Delta y)^2[(\frac{\partial u}{\partial y})^2 + (\frac{\partial v}{\partial y})^2]^{\frac{1}{2}}$$

These expressions are based on a previous formulation by Smagorinsky *et al.* (1965). The constant C_k, is an empirical quantity while Δx and Δy are the grid distances along the x and the y directions.

The fourth item represents the physical process which generates upslope motions during the daytime and downslope motions at night.

The expressions for $(\frac{\partial u}{\partial t})_s$ and $(\frac{\partial v}{\partial t})_s$ are:

$$(\frac{\partial u}{\partial t})_s = C_B g \frac{\partial h}{\partial x}(\theta_s - \theta)/\theta$$

$$(\frac{\partial v}{\partial t})_s = C_B g \frac{\partial h}{\partial y}(\theta_s - \theta)/\theta$$

Here, C_B is an empirical constant while θ_s is the temperature of the ground surface.

Next we discuss the prediction equation for θ (Eq. 3). Note that, in this equation, there are four physical processes which are parameterized. The first of these represents the horizontal diffusion of heat (the two terms involving K_x and K_y). The second process represents radiative temperature changes $(\frac{\partial \theta}{\partial t})_R$. The expression for this term is based on the concept of Newtonian cooling. Thus,

$$(\frac{\partial \theta}{\partial t})_R = C_R[0.9(T_s - T) + 0.1(T_D - T)]$$

Here, C_R, is an empirical constant while

T, temperature at surface anemometer level

T_s, ground surface temperature

T_D, temperature at $Z = D$.

The third term is intended to parameterize temperature changes due to vertical motion; e.g., cooling due to expansion when the motion is upward. The formula for this term is:

$$(\frac{\partial \theta}{\partial t})_W = -K_T \frac{\theta_D - \theta}{D - h}(V \cdot \Delta h) + K_c(\theta_D - \theta)(\frac{\partial u}{\partial x} + \frac{\partial v}{\partial y})$$

The first term on the right-hand side represents the effect of orographically-forced vertical motion; the second term represents the effect of vertical motions associated with surface convergence over flat terrain. Here, K_T and K_C are empirical constants.

The last process which is parameterized is the temperature change due to the flux of sensible heat from the Earth's surface $(\frac{\partial \theta}{\partial t})_Q$. In order to estimate this quantity, we assume that:

$$\theta(x,\ y,\ \sigma,\ t) = \bar{\theta}(\sigma) + \theta'(x,\ y,\ \sigma,\ t) \tag{5}$$

where $\bar{\theta}(\sigma)$ is the vertical variation of the prevailing large-scale potential temperature. Furthermore, we note that, at a particular point (x, y) and at any level, σ,

$$(\frac{\partial \theta}{\partial t})_{Q,\ \sigma} = (\frac{\partial \theta'}{\partial t})_{Q,\ \sigma}$$

We now make the important assumption that the vertical distribution of the heating is approximated by:

$$(\frac{\partial \theta'}{\partial t})_{Q,\ \sigma} = (\frac{1 - \sigma}{1 - \sigma_a})^n (\frac{\partial \theta'}{\partial t})_{Q,\ a}$$

Here the subscript, a, refers to values at surface anemometer level; the exponent, n, is an empirical constant. This assumption is based primarily on experience, similar to the power law for wind profiles. From here on, we will drop the subscript, a, from $(\frac{\partial\theta'}{\partial t})_{Q,\ a}$ for the sake of simplicity in notation. Having done that, we will now attempt to express $(\frac{\partial\theta'}{\partial t})_Q$ in terms of the sensible heat flux, Q, from the Earth's surface. In order to do this, the first step that is done is to integrate the equation above from the surface to the top of de domain. Thus,

$$\int_0^1 (\frac{\partial\theta'}{\partial t})_{Q,\ \sigma} d\sigma = (\frac{\partial\theta'}{\partial t})_Q (1-\sigma_a)^{-n} \int_0^1 (1-\sigma)^n d\sigma$$

Performing the integration and then solving for $(\frac{\partial\theta'}{\partial t})_Q$ one gets:

$$(\frac{\partial\theta'}{\partial t})_Q = (1-\sigma_a)^n (n+1) \int_0^1 (\frac{\partial\theta'}{\partial t})_{Q,\ \sigma} d\sigma$$

Note, however, that the integrand represents the total heating of the air column due to sensible heat flux. Therefore,

$$\int (\frac{\partial\theta'}{\partial t})_{Q,\ \sigma} d\sigma = \frac{Q}{D-h}$$

Combining this equation with the preceding, one gets:

$$(\frac{\partial\theta'}{\partial t})_Q = \frac{(n+1)(1-\sigma_a)}{D-h} Q \approx \frac{n+1}{D-h} Q = (\frac{\partial\theta}{\partial t})_Q$$

Finally, the heat flux (Q) must be expressed in terms of u, v, σ, and the surface temperature, θ_s. On the basis of the so-called bulk aerodynamic method, the formula is:

$$Q = C_D (u^2 + v^2)^{\frac{1}{2}} (\theta_s - \theta) \tag{6}$$

The drag coefficient (C_D) is, in turn, formulated in terms of the Richardson number (R_i) and the roughness parameter (Z_0), following a suggestion by Louis *et al.* (1981). The formula is:

$$C_D = \begin{cases} C_{DN}/[1+15Ri(1+5Ri)^{\frac{1}{2}}], & Ri>0 \\ C_{DN}\{1-15Ri/[1+75C_{DN}(-Ri\frac{Z_a}{Z_o})^{\frac{1}{2}}]\}, & Ri\leq 0 \end{cases}$$

where

$$C_{DN} = [k_o / ln(Z_a/Z_o)]^2$$

$$R_i \equiv Z_a g (\frac{\theta}{\theta_s} - 1)/(u^2 + v^2)$$

Here, k_o is the Karman constant, Z_a is the height of the surface observations for wind and temperature. The quantity, C_{DN}, is the customary value of the drag coefficient for neutral stratification.

The last important aspect of the model formulation which will be discussed is the determination of the geopotential of the surface anemometer level, ϕ_a. This is done by integrating the hydrostatic equation from the top of the model domain (σ_D) to the surface anemometer level (σ_a). In connection with the integration, one has to specify the vertical distribution of θ'. For this purpose, we make the same power law assumption which was made previously. Thus,

$$\theta'_\sigma = \theta'_a(\frac{1-\sigma}{1-\sigma_s})^n$$

Again, we will drop the subscript, a, in θ_a (for simplicity of notation) with the understanding that θ refers to the surface anemometer level. We note further that:

$$\theta_\sigma = \theta'_\sigma + \bar{\theta}(\sigma)$$

with θ'_σ given by the preceding formula. Substituting this in the hydrostatic equation, Eq. (4), and integrating, we get

$$\phi \equiv \phi_a = \phi_D + g(D-h)[\alpha - \frac{\beta\theta'}{(1-\sigma_a)^n}]$$

$$\alpha \equiv \int_{\sigma_a}^{1} \frac{1}{\theta(\sigma)} d\sigma$$

$$\beta \equiv \int_{\sigma_a}^{1} \frac{(1-\sigma)^n}{[\theta(\sigma)]^2} d\sigma \tag{7}$$

We have now finished the formulation of the model. The primary difference between the present model and the previous models of Danard (1977) and Mass and Dempsey (1985) lies basically in the assumption concerning the distribution of the potential temperature between the surface and the top of the model or the reference level. At this level, the amplitude of the mesoscale disturbance is assumed to be negligible; therefore, the values of u, v, θ and ϕ are the same as the values of the prevailing flow at the level.

The integration of the model requires the specification of the initial conditions for the horizontal distribution of u, v and θ at the surface anemometer level:

$$u(x,\ y),\ v(x,\ y) \text{ and } \theta(x,\ y) \text{ at } t = 0$$

In general, these correspond to the observed values of these quantities. The values are modified so that the initial flow is balanced geostrophically. However, they could be values which correspond to those of the prevailing flow at the surface anemometer level. In addition, it requires the values of ϕ at the reference level, ϕ (x, y, D) and the vertical distribution of θ corresponding to the

large-scale flow; i.e.:

$$\theta(Z) = \theta(Z), \quad h \leq Z \leq D$$

$$\theta(\sigma) = \bar{\theta}(\sigma), \quad 0 \leq \sigma \leq 1$$

With regard to lateral boundary conditions, we determine the boundary values at each time step according to the following convention:

a. At inflow points, the values are held constant.

b. At outflow points, the values are predicted, following the same procedure used at interior points.

In addition to these properties of the flow pattern, we also need to specify the following characteristics of the terrain:

a. Terrain roughness, $Z_o(x, y)$.

b. Terrain elevation, $h(x, y)$.

c. Surface temperature, $\theta_s(x, y, t)$.

A numerical integration is done by using the following step-by-step procedure:

1. Using the specified values of θ and $\bar{\theta}$ at surface anemometer level, compute the corresponding value of θ'.

2. Using this value of θ' in conjunction with Eq. (7), compute ϕ.

3. Compute the local tendency terms, $\frac{\partial u}{\partial t}$ and $\frac{\partial v}{\partial t}$ (Eqs. (1) and (2)).

4. Using the computed values of $\frac{\partial u}{\partial t}$ and $\frac{\partial v}{\partial t}$ calculate new (forecast) values of u and v for a short time interval, Δt.

5. Compute the heating term, Q, using Eq. (6).

6. Compute the temperature tendency, $\frac{\partial \theta}{\partial t}$, in Eq. (3).

7. Using this value of $\frac{\partial \theta}{\partial t}$, calculate the new (forecast) value of θ corresponding to the value after the short time interval, Δt.

8. Using the forecast values of u, v, and θ obtained in steps (4) and (7), repeat steps (1) to (7). Continue this repetitive procedure until the sum of the Δt's is equal to the desired range of the forecast.

3. Initial applications of the model

In order to illustrate the potential applications of the model, we present three examples of model simulations. These simulations correspond to the following phenomena:

1. Daytime flow induced by an isolated hill (no prevailing wind).

2. Modification of thermally-stable flow by an isolated hill (strong prevailing wind).

3. Manila Bay sea breeze (no prevailing flow).

In connection with the numerical integrations of the model, we replaced the differential equations by finite difference analogs. The finite differencing method is based on the forward (in time), upstream difference technique. A rectangular grid with a grid distance of 10 km is used. The time increment is 300 seconds. In all the simulations, the initial values of u, v, and θ are specified such that the wind field is balanced geostrophically. The other parameters and empirical model constants used in the integrations are: $D = 2$ km; $C_m = 6 \times 10^{-2}$; $S = 0.5$; $C_n = 35$; $C_K = 1 \times 10^{-4}$; $C_B = 0.0$; $C_R = 3 \times 10^{-5}$; $K_t = 1.0$; $K_c = 0.05$; $n = 0.1$; Z_o (land) = 10 cm; Z_o (sea) = 0.01 cm; $Z_a = 10$ m. The values of the empirical constants have been determined mainly by means of numerical experiments. This is done by integrating the model equations several times, using different values of any particular constant. The value of that particular constant which gives the most realistic integration is selected. They may not yet be the optimum values which should be used universally.

The first simulation, Item (1) represents an attempt to reproduce the mesoscale circulation which develops in the vicinity of an isolated hill as a result of surface heating during the daytime. The terrain elevation used in the simulation is given by,

$$h(x,\ y) = h_{\max}[e^{-[(x-x_o)^2+(y-y_o)^2]/L^2}]$$

where $h_{\max} = 1$ km, $L = 20$ km, and x_o and y_o represent the coordinates of the hill summit. In order to duplicate the diurnal surface heating at daytime, we specified the surface temperature to vary with time according to the following expression.

$$\theta_s(x,\ y,\ t) = 299 + 10 \sin \frac{2\pi t}{24}$$

with $t = 0$ at 8:00 a.m. local time. Assuming the initial time as 8:00 a.m., together with a prevailing flow which corresponds to calm conditions ($t = 0$, $u = 0$, $v = 0$), the equations were integrated for a time period which corresponds to 6 hours of meteorological time. The computed flow field at the end of this period (2:00 p.m.) is shown in Fig. 2, together with the contour heights of the terrain, $h(x, y)$. It may be seen that the hill has induced upward motions toward the summit. This flow pattern is in reasonable agreement with the observed upslope motions during the daytime, frequently resulting in cloud formation over hills. The maximum wind speed found on the hillside is approximately 8 ms^{-1}

The second simulation represents an attempt to reproduce the blocking effect of a hill on a strong prevailing flow if the thermal stratification of the prevailing synoptic condition is stable ($\frac{\partial \theta}{\partial Z} > 0$). In this simulation, we assumed the prevailing flow to have a speed of 20 ms^{-1} (at $t = 0$, $u = 20$ ms^{-1}; $v = 0$). The surface temperature was held constant with time at 299°K ($\theta_s = 299$°K); the corresponding lapse rate was specified as $\frac{\partial \theta}{\partial Z} = 25$°/km, a very stable thermal stratification. With these initial conditions and the same terrain used in the first simulation, we integrated the equations again for a period of 6 hours of meteorological time. The resulting flow field is shown in Fig. 3, together with the contour heights of the terrain. It may be seen that the hill tends to block the prevailing flow. Not that the flow appears to go around the hill, with a stagnation point on the windward side of the hill. On the leeside, strong winds are generated by the hill with maximum speed of about 30 ms^{-1}. The tendency for the prevailing flow to go around hills under stable stratification conditions is frequently observed in the real atmosphere.

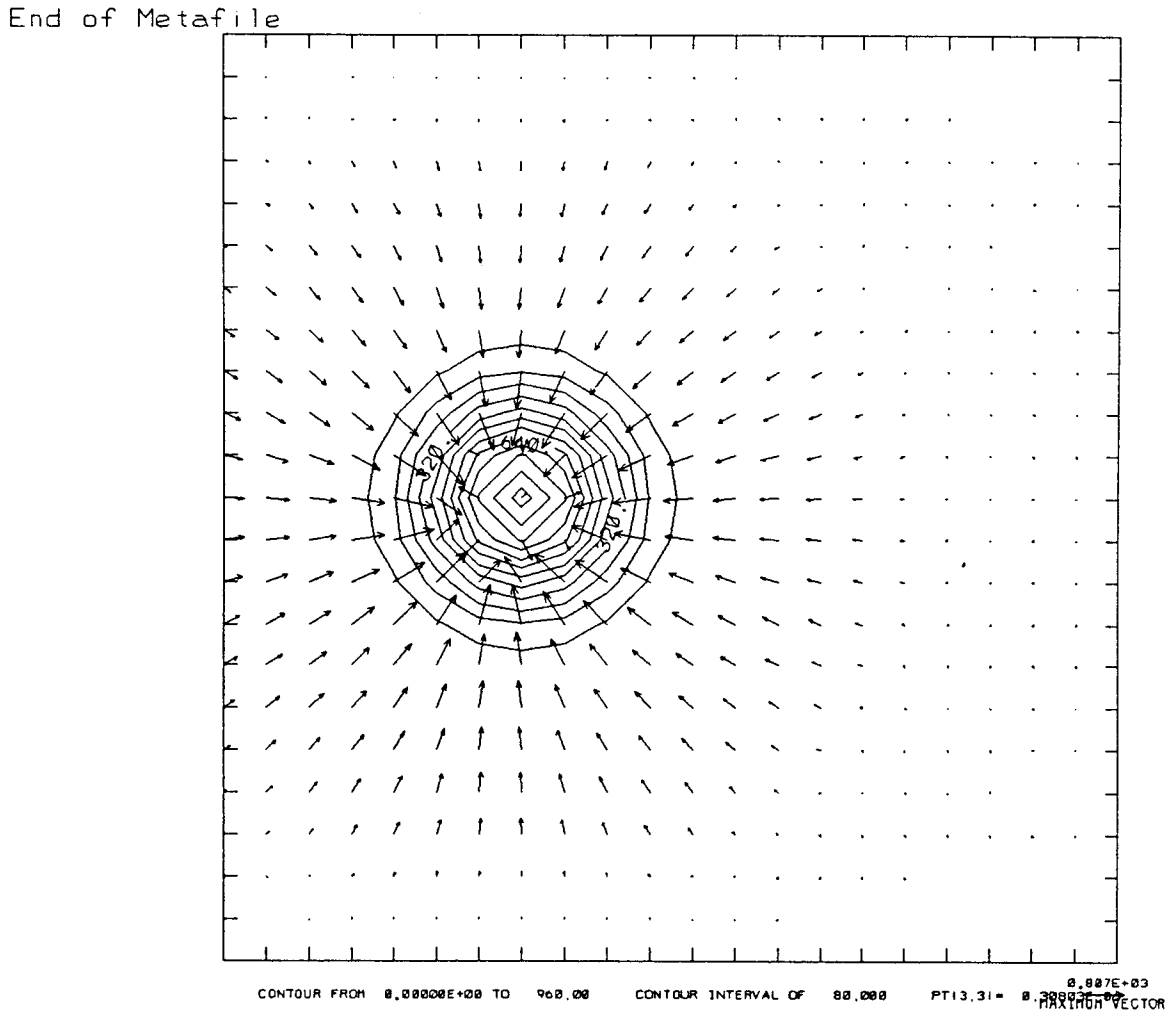

Fig. 2. Simulation of the flow pattern induced by an isolated hill during the daytime. The length of the wind vectors is proportional to the wind speed. The maximum wind speed is 8 ms^{-1}. The terrain heights are indicated by the contours; the contour interval is 80 meters.

In the third simulation, we have attempted to reproduce the sea breeze development in the vicinity of Manila Bay. The Manila Bay coastline is fairly complicated. In addition to this complication, there is another water body nearby toward the southeast Laguna de Bay. For simplicity, we assumed the topography to be flat, $h(x, y) = 0$ in the entire domain. The land surface was heated according to the equation for surface temperature in the first simulation; the sea temperature was held constant at 299°K. The large scale prevailing flow is zero ($t = 0$, $u = 0$, $v = 0$); the corresponding lapse rate of the flow is assumed to be given by $\frac{\partial \theta}{\partial t} = 5°/\text{km}$. Starting at 8:00 a.m., as the initial time, we integrated the equations for a period of 8 hours of

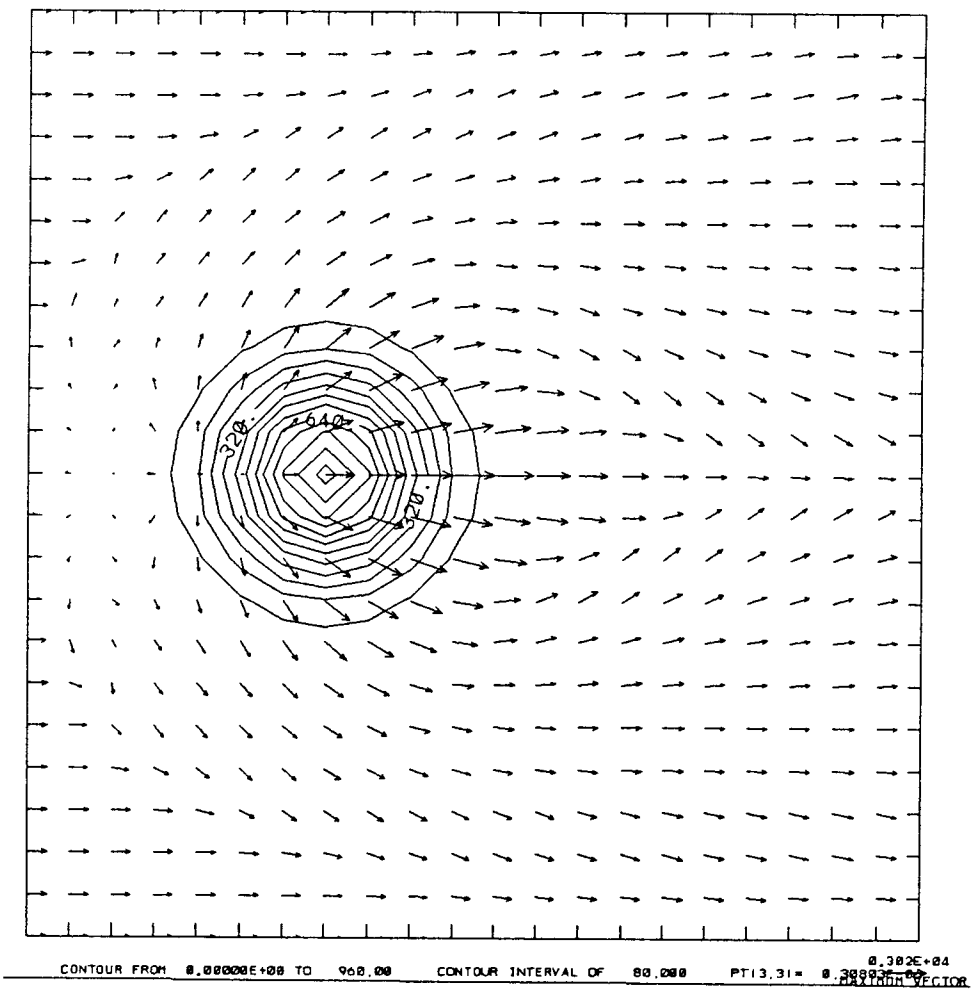

Fig. 3. Simulation of the flow pattern induced by an isolated hill under conditions of stable thermal stratification. The length of the wind vectors is proportional to the wind speed. The maximum wind speed is 30 ms $^{-1}$. The terrain heights are indicated by the contours; the contour interval is 80 meters.

meteorological time. The flow patterns at 12:00 Noon and at 4:00 p.m. are shown in Figs. 4 and 5. The shorelines are indicated by the lines whose contour value is 5.00. Looking at Fig. 5 first, we see that the wind field is characterized by flow towards land in the coastal areas; this is the sea breeze. The strongest winds (about 8 ms^{-1}) are located generally about 10 km inland from the shoreline. Farther inland, the wind speeds decrease, becoming zero at about 30 to 40 km distance from the shoreline. This distance represents the leading edge of the sea breeze (or depth of penetration) at 12:00 Noon. Note that, at this time, weak winds prevail over the center of Manila Bay.

Looking next at the wind field at 4:00 p.m. (Fig. 5), we see that the sea breeze has penetrated much farther inland towards the northeast (upper right hand of the figure). The maximum

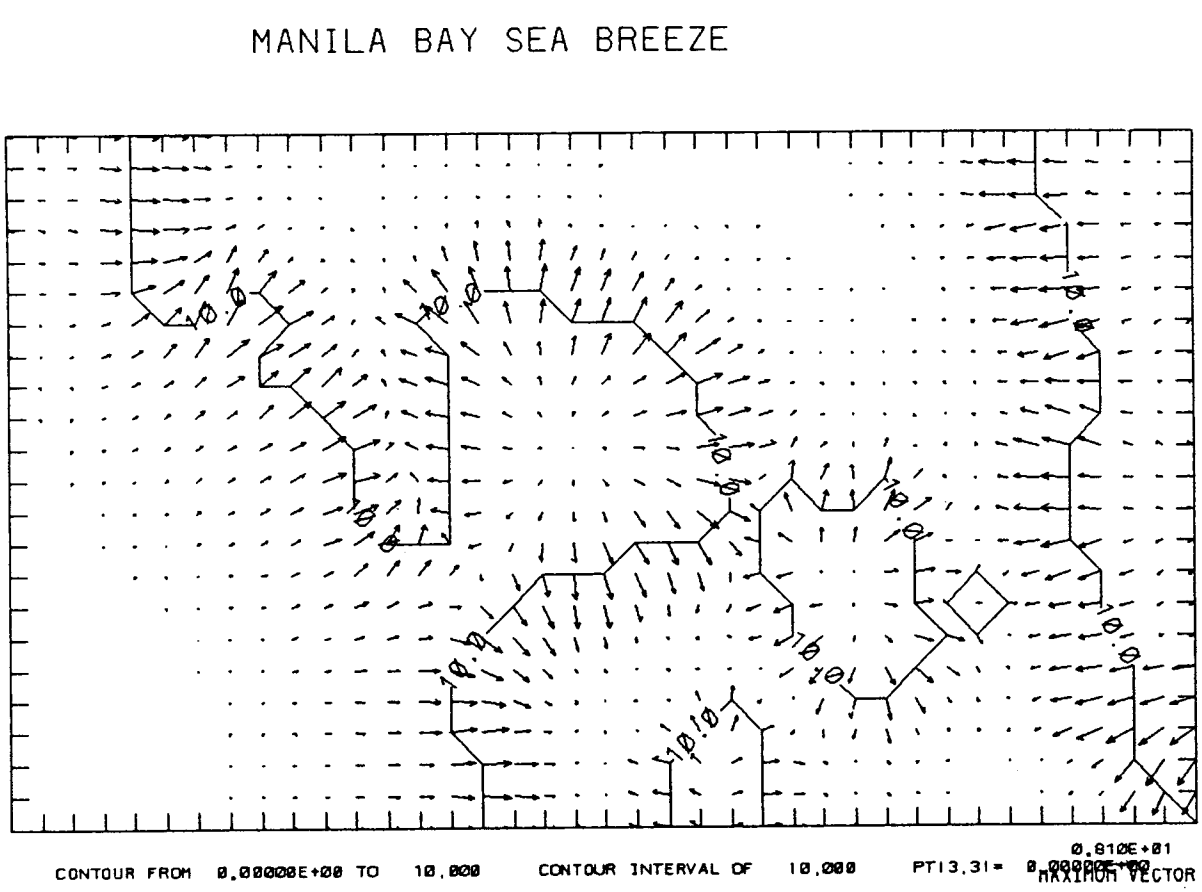

Fig. 4. Simulation of the sea breeze over the Manila Bay region and vicinity at 1200 LCT. The shoreline corresponds to the line which is labeled by the 5.00 contour. The length of the wind vectors is proportional to the wind speed. The maximum speed is 8 ms^{-1}.

wind speeds at this time are about 10 ms^{-1}. There are lines of convergence due to sea breeze components induced by coastlines with different orientations. Note, for example, the convergence line over the land south of Manila Bay. It may be seen also that the sea breeze circulation has expanded significantly over the sea areas. This expansion has resulted in southwesterly winds over Manila Bay, including the areas outside the bay towards the southeast.

The computed wind distributions for the sea breeze at 12:00 Noon and at 4:00 p.m. shown in these two figures appear to be qualitatively realistic. However, it must be recalled that the terrain has been assumed to be flat in the present integration. In reality, the terrain is quite complex, especially in the land area, west of Manila Bay (Bataan Peninsula). Consequently, the sea breeze simulation in this area may be rather unrealistic. In the future, we plan to make simulations which would take into account the effect of topography by specifying the proper terrain elevation, $h(x, y)$.

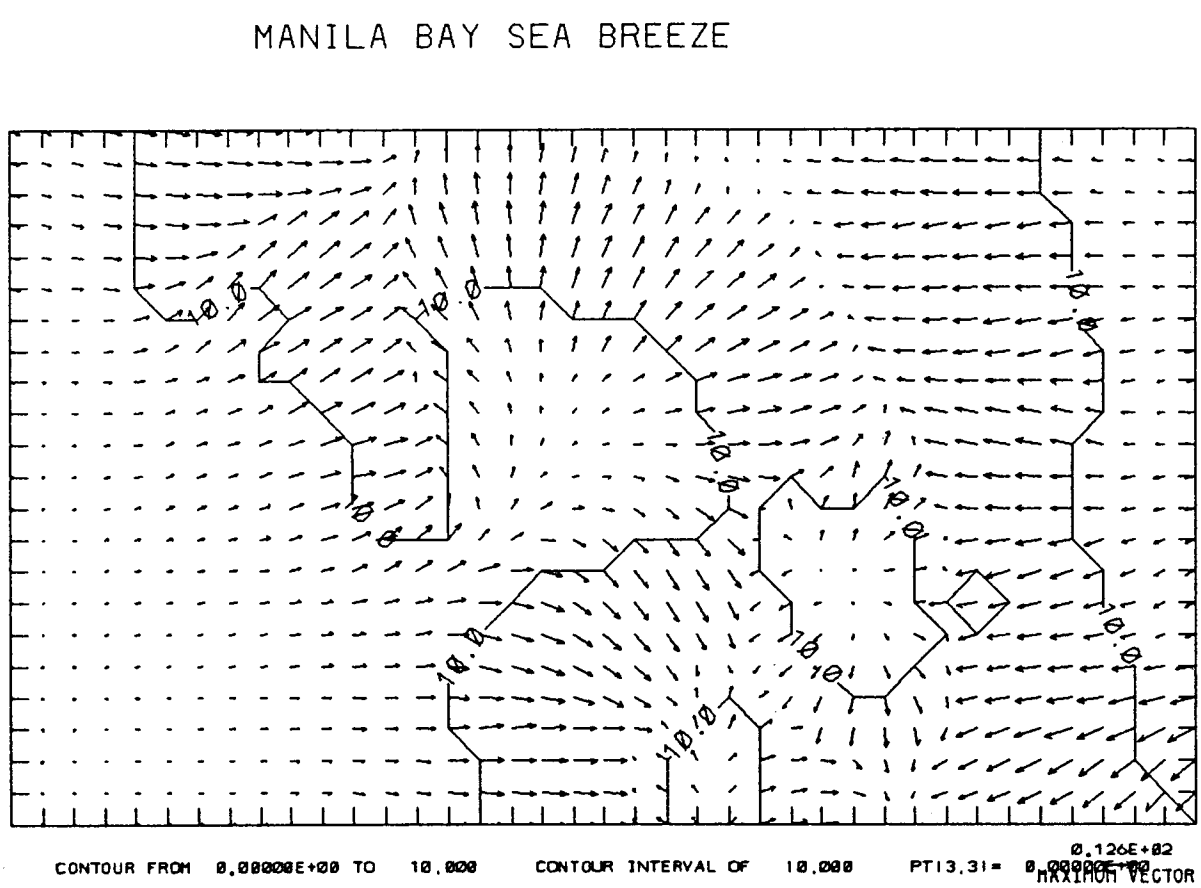

Fig. 5. Same as in Fig. 4 except for 1600 LCT. The maximum wind speed is 12 ms^{-1}.

4. Concluding remarks

In this paper, we have described a simple model which can simulate the perturbing effects of complex terrain on the large scale prevailing flow. Nonuniformities in terrain elevation as well as in surface temperature and roughness are incorporated in the model formulation. The model is two dimensional, describing only the horizontal distributions of the wind and temperature fields at the surface and their time variations. The effects of atmospheric conditions above the surface are parameterized. Consequently, the model is characterized by a relatively large number of parametric constants. This weakness is, however, compensated by the simplicity of the model equations. This simplicity makes it possible to integrate the equations by using only a personal computer. The results of applying the model for simulating the effects of topography (isolated hill) and nonuniform surface temperature (sea breeze phenomenon) are presented. The results are very encouraging, indicating that the model may have potential use in the study of mesoscale disturbance over complex terrain.

Acknowledgements

The research has been partially supported by a grant from the National Science Foundation (International Section, Grant No. 8709973) through the Clean Energy Institute of The University of Miami.

REFERENCES

Danard, M., 1977. A simple model for mesoscale effects of surface winds. *Mon. Wea. Rev.*, **105**, 572-580.

Estoque, M. A. and J. Gross, 1981. Further studies of a lake breeze. Part II: Theoretical Study. *Mon. Wea. Rev.*, **109**, 213-228.

Lavoie, R. L., 1972. A mesoscale model for lake-effect storms. *J. Atmos. Sci.*, **219**, 1025-1040.

Louis, J. F., M. Tiedtke and J. F. Golga, 1981. A short history of PBL parameterization at ECMWF. Workshop on Planetary Boundary Layer Parameterization, ECMWF, Reading, Berkshire, England.

Mass, C. F. and D. P. Dempsey, 1985. A one-level mesoscale model for diagnosing surface winds in mountainous and coastal regions. *Mon. Wea. Rev.*, **113**, 1211-1227.

Smagorinsky, J., S. Manabe and J. L. Holloway, 1965. Numerical results from a nine-level general circulation model of the atmosphere. *Mon. Wea. Rev.*, **93**, 727-742.